Study of Mode I Fracture of Self Assembled Monolayers with ABAQUS

EM 388F Term Paper

Instructor: Dr. Huang

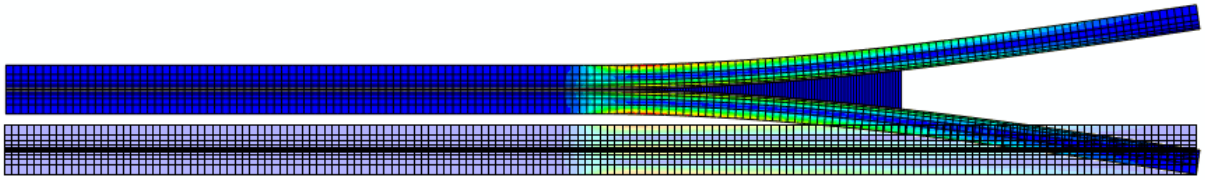

by

Masayuki Wakamatsu

Department of Aerospace Engineering and Engineering Mechanics

The University of Texas at Austin

May 9, 2008

Abstract

A numerical study of interfacial fracture of self assembled monolayers in mode I configuration was considered. If adherents are bonded with a thin layer to form a DCB specimen, and are subjected to mode I type loading, interfacial fracture toughness is governed by the intrinsic toughness of bonded interface that can be presented as traction separation law. For the numerical study, ABAQUS vr. 6.7.1 was used to model and assess DCB specimen. DCB was consisted of 0.32mm thick silicon wafers, bonded by self assembled monolayers. As a base of traction separation property of adhesives, the maximum traction was designed as 1.0 MPa, and the maximum separation length was 200 nm. Due to the limitation of ABAQUS cohesive element definition, only triangular shape of traction separation properties was considered. This problem was considered as large scale bridging; thus, a shape of traction separation properties greatly affected the response of reaction load and input displacement resultant curves. When keeping the interfacial fracture toughness constant, and increase the slope of traction separation property, the load required to propagate a crack decreased significantly. Increasing the toughness resulted in increase in load required to propagate the crack. In both cases, LEFM predictions gave offset but somewhat admissible results. Shortening the separation length in traction separation property resulted in increase in loading slope.

Table of Contents

1.0 Introduction

In EM 388F, history and theories of fracture mechanics were discussed. As a final project, interface fracture behaviors driven by different properties of traction separation will be discussed. Specifically, a double cantilever beam, DCB, sandwich specimen made of silicon, bonded by self assembled monolayers, and subjected to mode I type loading is considered. Self assembled monolayers, SAMs, are consisted of one molecular length, 2 to 3 nm, of ordered molecules that are self assembled onto the substrate surface in ordered manner (Ulmann, 1996). SAM can be broken down to Head group, body, and tail group, Figure 1a. When a substrate is submerged into a solution containing molecules, a SAM is attracted to the surface and attached on the surface. Figure 1b shows a schematic on Si-H substrate and one molecule.

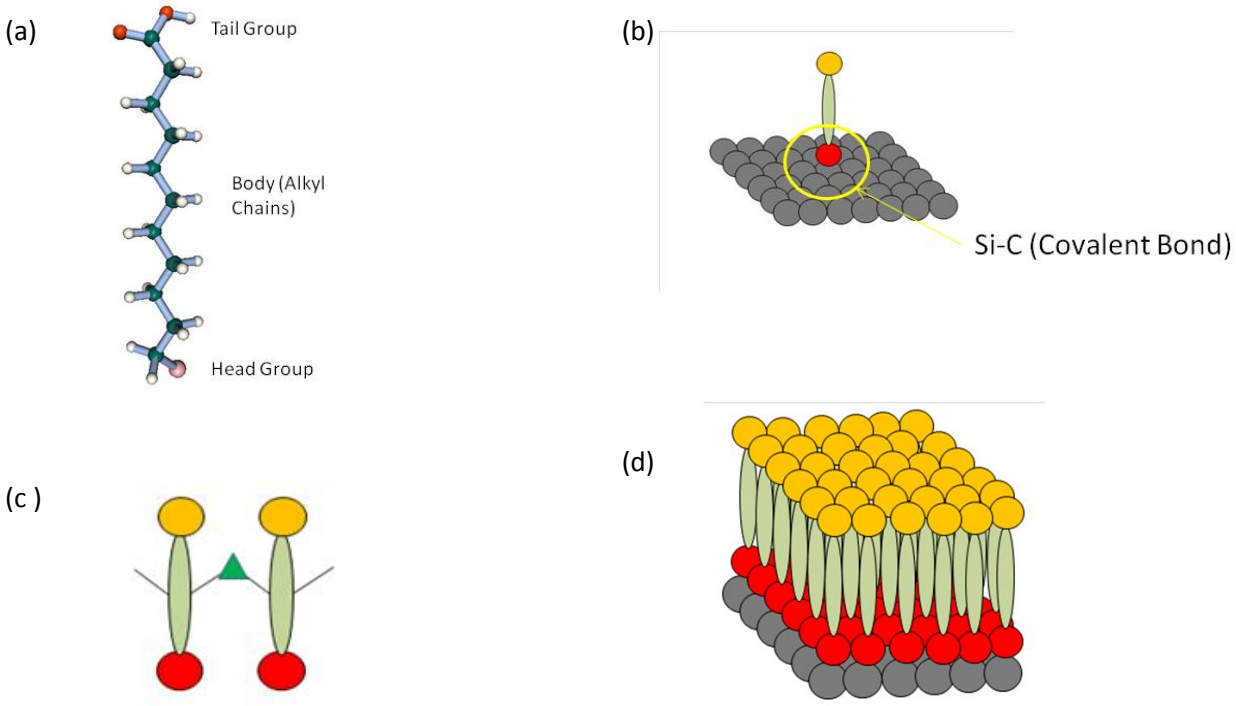

Figure 1: Self Assemble Monolayer (a) Example of Self Assembled Monolayer,
(b) Schematics on how SAM is bonded to a substrate
(c) van der Waals interaction between SAMs
(d) Surface Coverage of SAM

Without a special treatment, SAMs will form on the substrate surface in ordered manner. As shown in Figure 1c, body, or alkyl chains, is attached to each other by van der Waals force; thus, the surface coverage of SAM coverage on the substrate surface results in so dense that it would be a good assumption to leave the surface coverage as another ultra thin layer on a substrate. By tailoring functionalities of tail

group, SAM surface can be sticky or non-sticky state, similar concept to hydrophobic or hydrophilic surface. In this study, sticky SAM is employed as ultra thin adhesive, specifically speaking, its thickness shall be considered as 2.0 nm.

Now consider those ultra thin surface is used as adhesives, and Si-SAM – SAM –Si DCB sandwich specimen is prepared. Swadener and Liechti suggested that interfacial fracture toughness depends greatly on the intrinsic toughness of interfaces (1998). The increase in intrinsic toughness theory, which claimed types of atomic bonding of an interface influenced the toughness of interfacial fracture toughness, was further validated by Mello with sticky SAMs to epoxy interface (2006). The objective of this study is to predict interfacial fracture energy of SAMs as a traction separation property. Assume that displacement is applied at the end of DCB, and then reaction load is measured. Since SAMs is negligibly thin, mode mix can be considered as negligible. In other words, a pure mode I interfacial fracture is studied. ABAQUS, Vr 6.7.1, is used to create and analyze the problem.

2.0 Theory

2.1 DCB Sandwich specimen (Mode I)

Figure 2 depicts the overview of mode I interfacial fracture testing. Δ is defined as a displacement applied at the end of DCB; P is a reaction force cased by this displacement input.

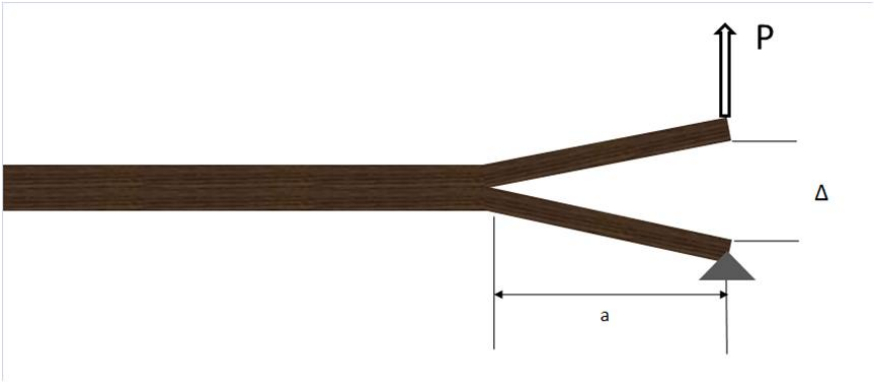

Figure 2: Configuration of Mode I type loading on DCB

From LEFM approach, Energy Release Rate at the crack tip, Gtip, can be defined as follows (Gdoutos, 2005)

$$G = \frac{\eta P^2 a^2}{EbI} \tag{1}$$

where

$$I = \frac{bh^3}{12} \tag{2}$$

Plane Strain

$$\eta = 1 - \nu^2 \tag{3}$$

Table 1: Dimension and Property of Si Beam

			Input is in yellow	
	m base unit		mm Unit	
Material Property		(unit)		(unit)
L	1.60E-02	m	16	mm
b	5.00E-03	m	5	mm
h	3.20E-04	m	0.32	mm
E	1.69E+11	Pa	1.69E+05	N/(mm^2)
nu	3.00E-01		0.22	N/A

A simple iterative Matlab coding was prepared with the dimensions and properties defined in Table 1 with Γ_0 equals to 0.1 J/m^2. Figure 3 shows the resultant P vs Δ curve.

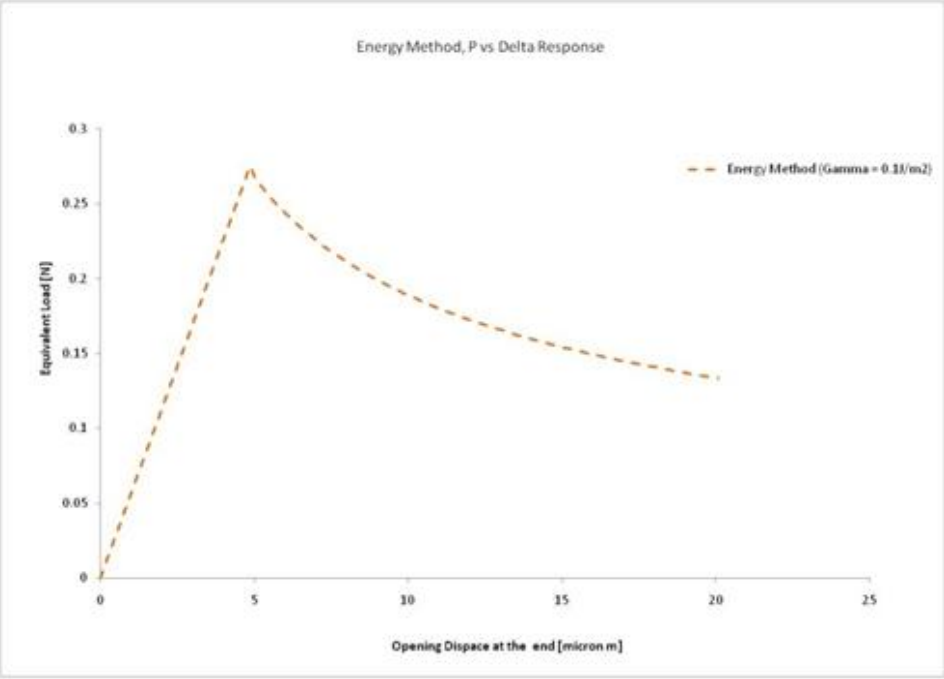

Figure 3: Theoretical P vs Δ from Energy Method

2.2 Traction Separation Law (Cohesive Zone Model)

In the past 40 years, cohesive/bridging zone interface materials, such as from atomic separation, ductile materials, and especially composites, were studied extensively (Bao and Suo, 1992). Unlike LEFM case, a cohesive zone model, CPZ, considers cohesive zone or damage zone at the crack tip. Consider atoms are about to be separated, the adhesion force tends to increase at certain distance, and once their distance reached to its maximum adhesion force, then attracting force decreases. Thus, this study assumes that a traction separation of SAMs behaves in triangular manner as shown in Figure 4. The maximum separation stress, σ_0, separation length at the maximum stress occurs, δ_0, and maximum separation length, δ_c, characterize the property. It is important to note that an interfacial traction separation behaviors in mode I, mode II, or mode III, are different each other. Detailed mixed mode delamination solutions are available (Parmigami and Thouless, 2007), but it would be beyond this scope this study; thus, it would not be mentioned here. In this case studies mixty is almost zero because SAM adhesive layer is thin compared to thickness of a substrate (Gdoutos, 2005).

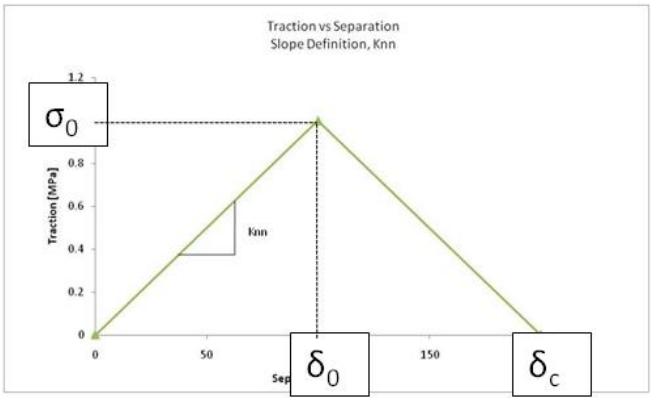

Figure 4: Example of Traction Separation Property

2.3 Small Scale Bridging and Large Scale Bridging

A traction separation model can roughly be divided into two groups, small scale bridging, SSB, and large scale bridging, LSB. Define "a" as a crack length and be a distance from end of DCB to the first existing cohesive element as shown in Figure 5. Similarly, let "L" be a cohesive zone, or bridging zone, which is a length between the most stretched to least stretched cohesive elements that are contributing to toughening a DCB specimen. As displacement is applied, L increases and reaches to Lss, then it will propagate the crack with a constant Lss, called steady state cohesive zone.

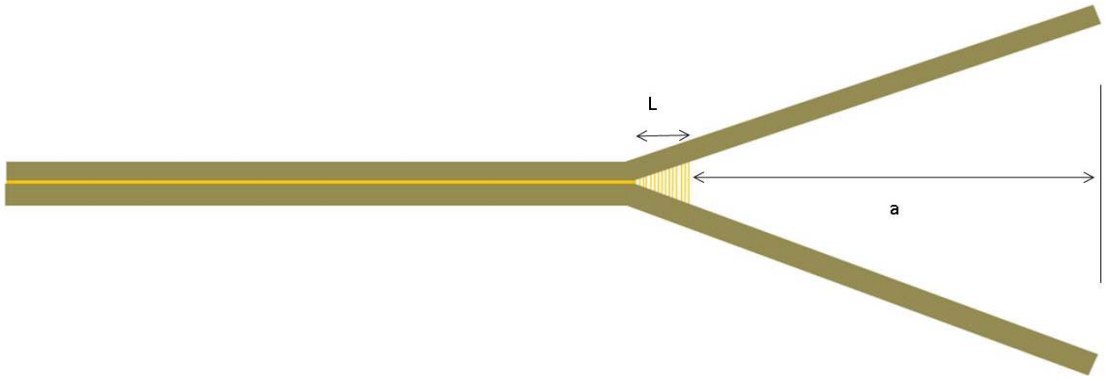

Figure 5: Definition of crack length (a) and Cohesive Zone (b)

Bao and Suo summarized definitions of SSB and LSB (1992). For SSB, a single material length is introduced as $\frac{\delta_c E}{\sigma_0}$; for LSB, a non dimensional parameter, $\frac{a}{\left(\frac{\delta_c E}{\sigma_0}\right)}$, was introduced, where a is a characteristic length of a problem, for instance a thickness of DCB (Bao and Suo, 1992). In case of SSB, the steady state damage zone is suggested as

$$L_{ss} = 0.366 \frac{\delta_c E}{\sigma_0} \tag{4}$$

LFEM solution does not consider any microscopic details of fracture process, but it provides good estimates in SSB case but is invalid in LSB case (Bao and Suo). For studying LSB phenomena, component geometry and traction separation property have to be coupled.

2.4 Abaqus Model

ABAQUS vr. 6.7.1 was used to model a 2D DCB model. Dimensions and properties used in the models are summarized in Table 1. Si substrate was modeled as plain strain condition with element CPE8R, an 8-node biquadratic plane strain quadrilateral, reduced integration. SAMs are modeled with a cohesive element, COH2D4, a 4-node two-dimensional cohesive element. MAXE damage criterion was used for damage propagation. The model consisted of 1,900 elements and 6064 nodes. To validate the meshing sides, convergence process was applied and rested this meshing model.

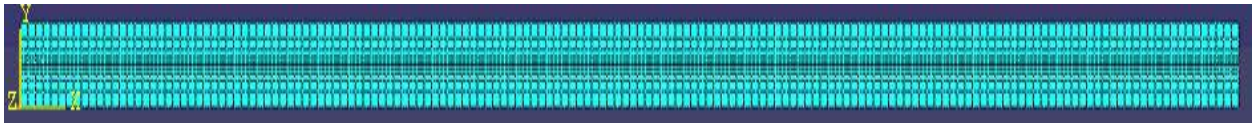

Figure 5: Overview of ABAQUS DCB Specimen Model

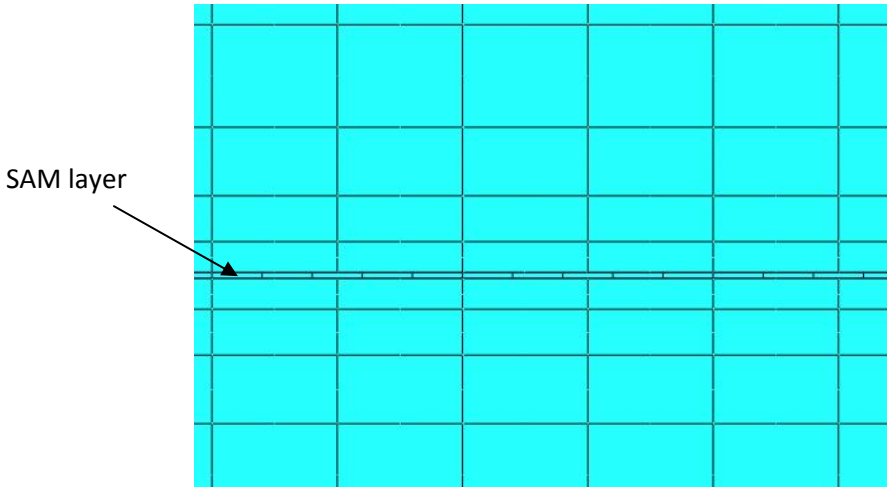

Figure 6: Close up on SAM in ABAQUS DCB Specimen Model

2.5 Case Studies – Parametric Characterization

The traction separation property of SAMs can be estimated from P vs Δ curve. To do so, one needs to understand to how traction separation properties such as maximum traction, σ_0, separation length at the maximum traction, δ_0, and the maximum separation, δ_c, affect the P vs Δ results. A several different traction separation properties, named as base X, are considered which are divided into three cases. Case1 considered how a slope of traction separation property would result in P vs Δ. Case 1 consists of five different slopes in traction separation property all of which possess the identical interfacial fracture energy, 0.1 J/m^2. Case2 assessed how different interfacial fracture energy would appear in resultant curve. Case 2 keeps the slope and separation length identical, but interfacial fracture energy was increased to twice or three times higher. Finally, Case 3 considered how the maximum separation length affects the loading result, keeping the interfacial energy constant, 0.1 J/m^2.

Table 2: Summary of all traction separation properties used in case studies

	Case 1	Case 2	Case 3	σ_0 [MPa]	δ_0 [nm]	δ_c[nm]	Γ_0 [J/m^2]	$\delta_c E/\sigma_0$ [mm]
Base 1	Y			1.00	200	200	0.1	33.80
Base 2	Y			1.00	150	200	0.1	33.80
Base 3	Y		Y	1.00	100	200	0.1	33.80
Base 4	Y			1.00	50	200	0.1	33.80
Base 5	Y	Y		1.00	5	200	0.1	33.80
Base 6		Y		2.00	10	200	0.2	16.90
Base 7		Y		3.00	15	200	0.3	11.27
Base 8			Y	1.33	75	150	0.1	19.06
Base 9			Y	2.00	50	100	0.1	8.45

Table 2 provides the summary of traction separation properties considered in all case studies. Similarly, Figure 8 shows the graphic representation of the input values.

Case 1

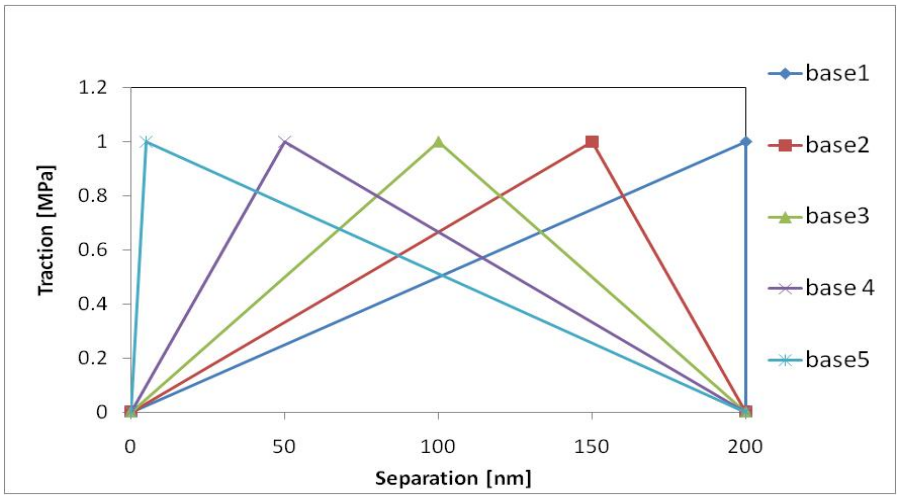

Case 2

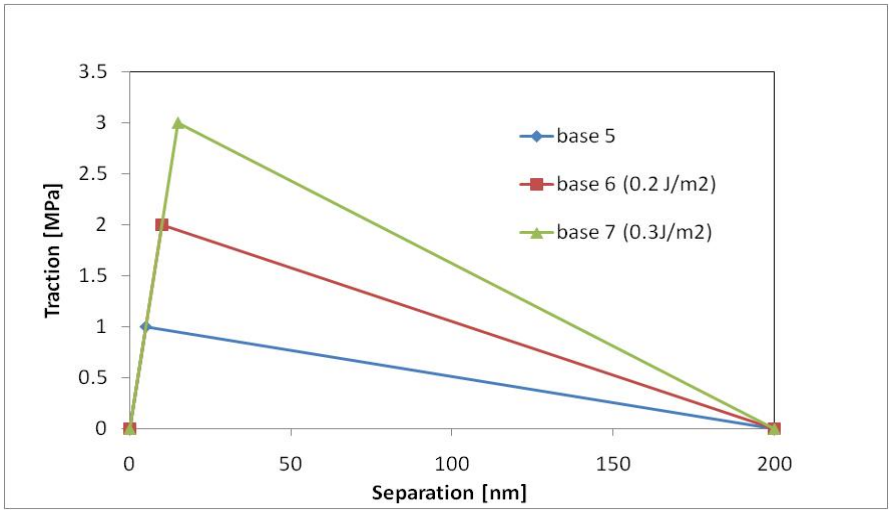

Case 3

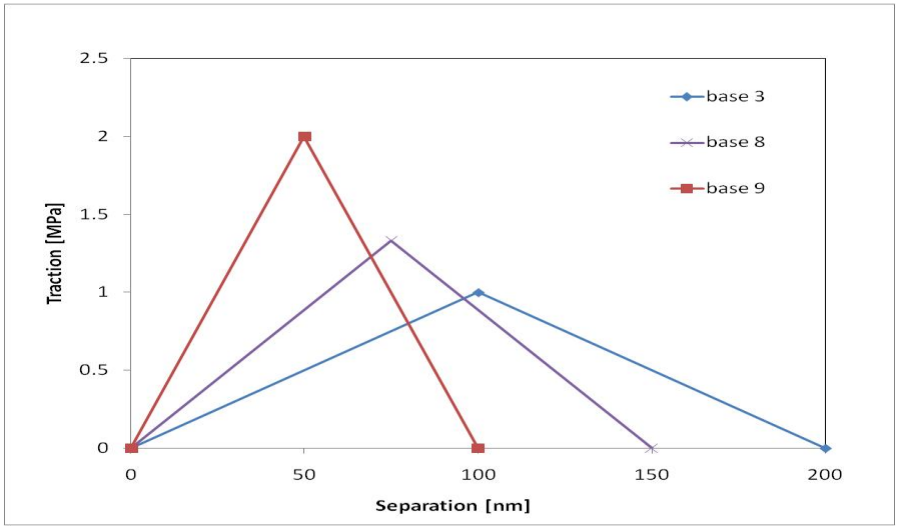

Figure 7: Traction Separation Properties of SAM for Each Case Study

3.0 Results

Before discussing the results of case studies, a single material length was calculated as 33.8 mm. This value is larger than a thickness of DBC, which was 0.32mm, and also larger compared to the initial crack length, 4.0 mm. Thus, the problem studied in this project can be classified as LSB problem.

Case 1. Same Fracture Energy, Different Slope

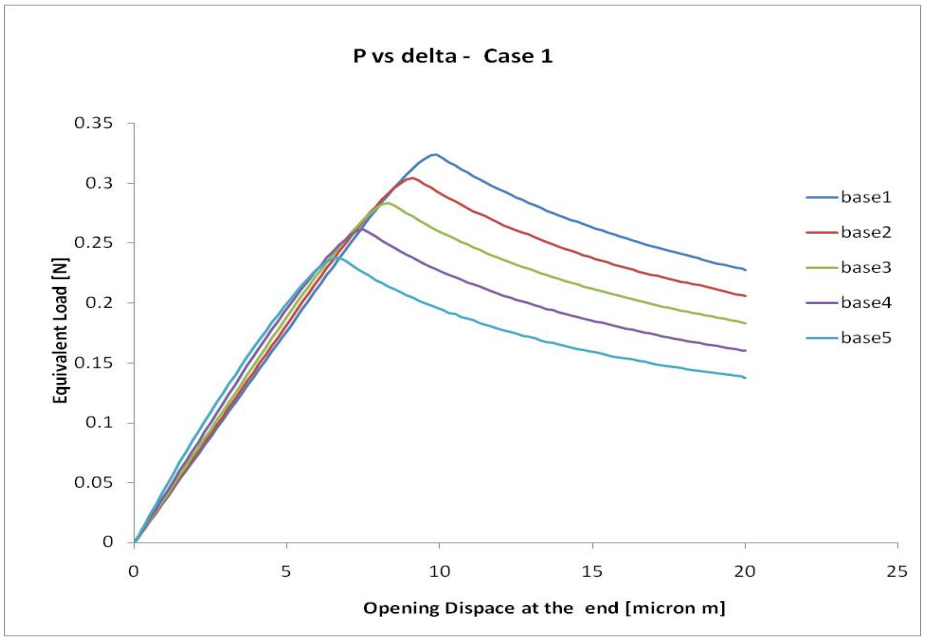

Figure 8: P vs Δ in Case 1 Study

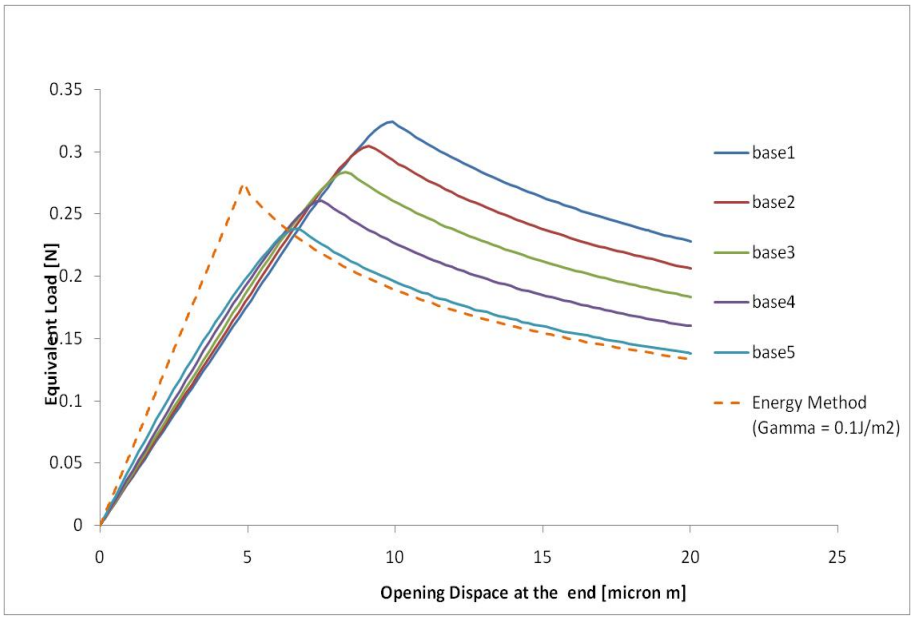

Figure 9: P vs Δ in Case 1 Study with LFEM solution

Figure 8 shows the results of Case 1 study. Two major trends were found. First, as a slope of traction separation property increases, the reaction load, P, decreased. In an extreme case, the maximum reaction load of Base 1 was higher by 40% than that of Base 5. Second, each traction separation slope showed an individual response similar to the maximum load values. Specifically speaking, the steeper the slope of traction separation property is, the lower the load necessary to propagate the crack. And the difference in load during the propagation region was constant in magnitude, or slope was similar, to all slopes considered. In addition, all five slopes were compared with LFEM case, Figure 9. Although all cases possessed the identical interfacial fracture energy, 0.1 J/m^2, LFEM prediction gave offset values but in the same order of magnitude.

Case 2: Same Separation Length, Increase in Interfacial Fracture Energy

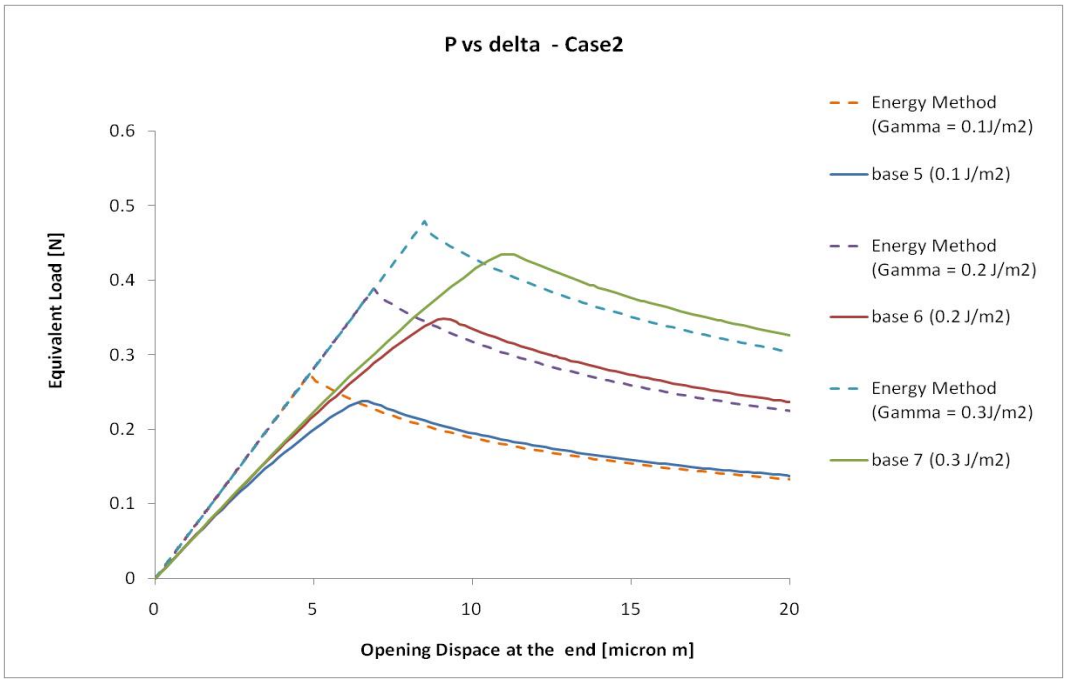

Figure 10: P vs Δ in Case 2 Study with LFEM solutions

As interfacial fracture energy was increased, both the reaction load and tip opening distance that required initiating the steady state cracking increased, Figure 10. LEFM solutions are also plotted in the same figure, and shows that their solution also increased as the interfacial fracture energy was set higher.

Case 3. Same Interfacial Fracture Energy, Shortening Max. Separation Length

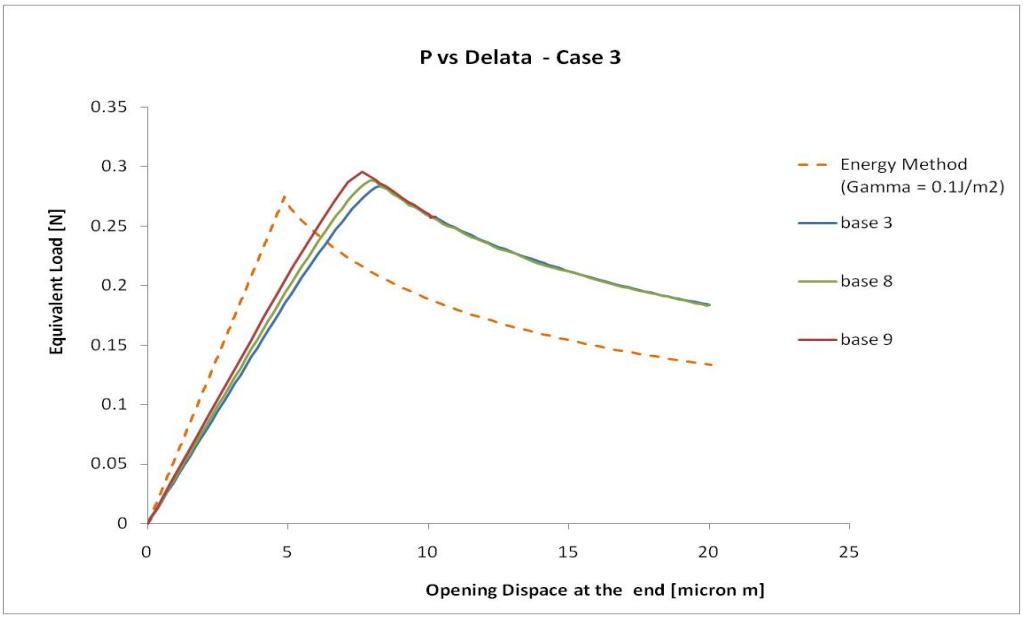

Figure 11: P vs Δ in Case 3 Study with LFEM solutions

Figure 11 depicts the resultant curve from Case 3. As the maximum separation length was shortened, the slope of the resultant curve increased. Also the maximum load became higher as the separation length shortened. Interestingly, although three bases have different slopes, the resultant curve followed what seems as asymptotic line. LEFM solution of 0.1 J/m^2 was also plotted in the figure, which did not exactly coincide with the asymptotic line of all three cases, but did show offset trend of P vs Δ resultant curve.

Fracture Propagation

In addition, a detail look on crack propagation and damage initiation and zone length evolution was studied for Base 1, Base 3, and Base 5 traction separation properties because they possessed the same interface toughness. A path was defined along the cohesive element so that crack opening distance and cohesive zone length can be evaluated. Figure 12 shows the crack length, a, as a function of time in second. Recall that input of ABAQUS model was opening displacement of 0.01 mm/s. It was found that as the slope of traction separation property increases, the crack propagation started earlier. Figure 13 shows the cohesive zone length against input opening displacement. Two major trends are noticeable.

First, as slope of traction separation property increases, the increase in cohesive zone length decreased. Second, the steady state cohesive zone was independent of slopes of traction separation curve.

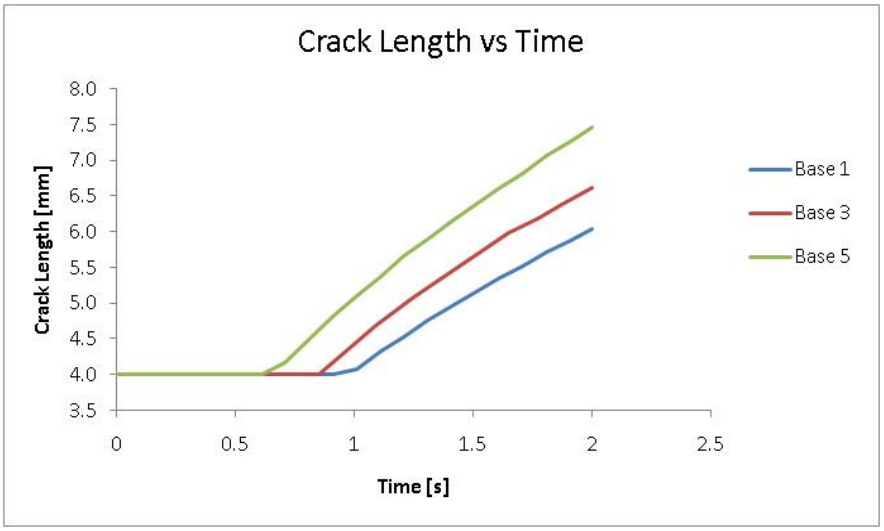

Figure 12: Crack length (a) vs time Case 3

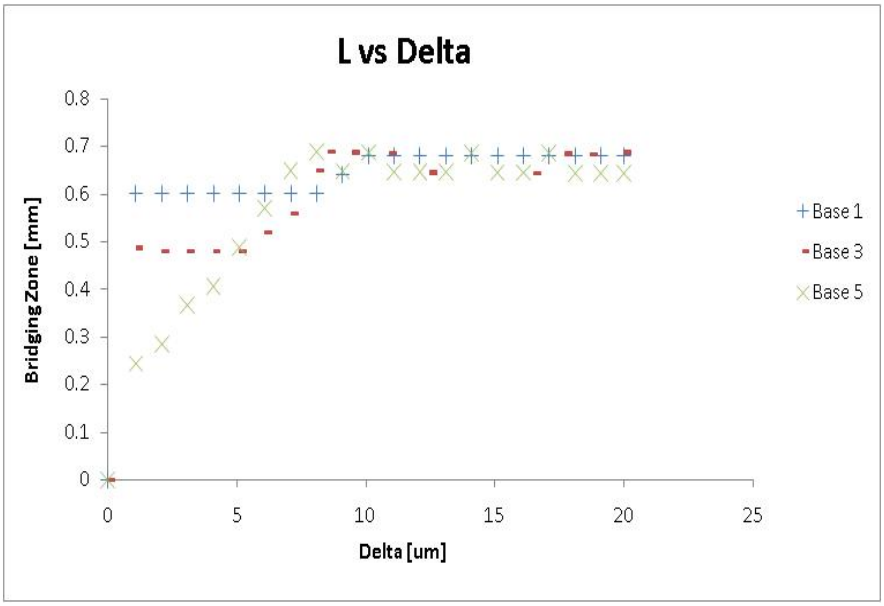

Figure 13: Bridging Zone vs Opening Distance

4.0 Conclusion

Parametric studies in property of traction separation law in interfacial fracture behaviors were considered. A finite element model with cohesive element as interface was developed with ABAQUS software. When keeping the interfacial fracture toughness constant but increasing the slope of traction separation property, the load required to propagate a crack decreased significantly. Increasing fracture toughness resulted in increase in load required to propagate the crack. In both cases, LEFM predictions gave offset but somewhat admissible results. Shortening the separation length in traction separation property resulted in increase in loading slope. With those results, once experimental data of P and Δ values become available, it would be possible to predict the traction separation property of SAMs. The author would like to suggest the following procedures: (i) With LEFM prediction, try to estimate the intrinsic fracture toughness, (ii) vary the slope of traction separation curve to correlate the empirical data, (iii) increase or decrease the separation length to align the slope of P vs Δ curve, and (iv) repeat (ii) and (iii) until satisfactory curve fitting is achieved.

5.0 Reference

Bao, G. Suo, Z. Ramarks on crack-bridging concepts. Appl. Mech. Rev. vol. 45. (1992)

Gdoutos, E. Fracture Mechanics 2nd Edition. Greece (2005)

Mello, A. Liechti, K. The effect of self-assembled monolayers on interfacial fracture. J. of App. Mech. Vol. 7. N5. 860-870. (2006)

Parmigiani, J. Thouless, M. The effects of cohesive strength and toughness on mixed-mode delamination of beam-like geometries. Eng. Frac. Mech. Vo. 74. PP 2645-2699. (2007)

Swadener, J. Liechti, K. Lozanne, A. The intrinsic toughness and adhesion mechanism in the mixed-mode fracture of a glass/epoxy interface. Journal of Applied Mechanics, 65, 25-29. (1999)

Ulman, A. Formation and Structure of Self-Assemble Monolayers. *Chemical Reviews* 96: 1533-1554, New York (1996)